

# Aerodynamic analysis of NACA SC (2) -0714 and NACA SC (2)-0414 super critical aero foils –a comparative study

M. Sri Rama Murthy<sup>1</sup>, K.Rambabu<sup>2</sup>

<sup>1</sup> Professor, Department of Mechanical Engineering, Sir C.R.Reddy College of Engineering, India

<sup>2</sup> Professor, Department of Mechanical Engineering, Sir C.R.Reddy College of Engineering, India

---

**ABSTRACT:** Supercritical aero foils are two dimensional turbulent aero with good transonic behavior while retaining acceptable low speed characteristics. In the Present work, comparisons are made between two super critical aero foils NACA SC (2) - 0714 and NACA SC (2) -0414 in the transonic range. Aero foils are modeled using CATIA V5 and analysis has been done with ANSYS Fluent software. Parameters observed are static pressure and velocity on both the aero foils at Mach numbers 0.7, 0.8, 1, and 1.2 with different angles of attack. It was observed that the flow is turbulent at Trailing edge than at Leading edge and the boundary layer separation is gradually increases at the given Mach number and angle of attack for both the aero foils. The drag and lift of both aero foils are studied with different mach numbers at different angles of attack. It was observed that lift coefficient of NACA SC (2) – 0714 is higher than that of NACA SC (2) -0414 and drag coefficient of NACA SC (2) – 0714 is comparable to NACA SC (2) -0414 at all Mach numbers and angles of attack. NACA SC (2) – 0714 super critical aerofoil was given a better performance than NACA SC (2) -0414 in this study.

**KEY WORDS:** Angle of Attack, Drag coefficient, Lift coefficient, Mach number, Super critical aero foils.

---

Date of Submission: 12-11-2022

Date of Acceptance: 26-11-2022

---

## I. INTRODUCTION

It is well known that the subsonic cruise speeds of high performance aircrafts are limited by onset of the transonic drag rise. The use of wing sweepback delays this onset of the transonic drag rise. However, for practical amounts of sweepback (approximately 35°) the onset still occurs well below the speed of sound i.e. between Mach numbers 0.80 and 0.85. One method for increasing the cruise speed further is the use of airfoil shapes which delay the drag rise.

The first airfoils developed in the U.S.A to delay the drag rise were the NACA 1 series airfoils. These airfoils designed to increase the Critical Mach number, that is, the Mach number at which supersonic flow first develops locally on the airfoil, have drag rise Mach numbers significantly higher than the earlier NACA four digit series airfoils. The NACA 6- series airfoils also provide increase critical Mach numbers with resulting improvements in the drag rise characteristics as compared with those for the 4-digit series.

Improvements to these early, phase 1 airfoils resulted in airfoils with significantly reduced drag creep characteristics. These early, phase 1 airfoils and the improved phase 1 airfoils were developed before adequate theoretical analysis codes were available and resulted from iterative contour modifications during wind-tunnel testing. Starting in the early 1970's, several such airfoils were developed. Emphasis was placed on designing turbulent airfoils with low cruise drag, high climb lift-to-drag ratios, high maximum lift, and predictable stall characteristics.

Ravi Kumar T and Dr.S.B.Prakash [1] conducted computational study of flow separation on super critical aerofoil NACA SC (2) 0714 at different angles of attack using CFD. In this work, the observed parameters are pressure drag, drag and lift coefficients at Mach number 0.6 and Reynolds number  $0.36 \times 10^6$ . It was concluded that no flow separation occurred at lower angles of attack due lower pressure gradient and flow separation started at AOA 15°, increases as the angle of attack increases. Also drag and lift coefficients are increased up to 20°, optimized at 20°.

Rubel R.I., et.al, [2] conducted experimental and numerical investigations to study the comparative performance of NACA 0015 and NACA 4415 aero foils. From this, it was concluded that the cambered aerofoil NACA 4415 is the most efficient aerodynamic shape than symmetrical aerofoil NACA 0015. For same area of NACA 4415 can produce higher lift coefficient than NACA 0015. Stalling takes place for NACA 0015 at between  $10^\circ < \alpha \leq 15^\circ$  AOA.

A comparative CFD analysis of NACA 2313 and NACA 7322 was carried out by M.Umapathi and Neelesh Soni [3] to find out efficient Aerofoil design. Analysis was performed at AOA 6° and 10° and

concluded that aerofoil NACA2313 is superior to NACA7322 as the ratio of coefficient of lift to coefficient of drag for NACA2313 aerofoil is higher than that of NACA7322 aerofoil.

Haydar Kepekci [4] conducted comparative numerical analysis of NACA 0015 and NACA 4415 aero foils at various angles of attack between 0 to 20 degrees using ANSYS Fluent software to know the performance. From this work, it was concluded that NACA 4415 with a cambered airfoil is more efficient than NACA 0015 with a symmetrical airfoil at every angle of attack.

CFD Analysis of RAE 2822 supercritical aerofoil was carried out by K.Harish Kumar et.al, [5] to improve the stability of aerofoil when the flow approaches the transonic Mach speeds. Here the performance of aerofoil has been done with and without wedge profiles along with the studies of lift and drag coefficients at different Mach numbers. It was concluded that the supercritical aerofoil with wedge profile is more stable and gives good performance at transonic Mach numbers.

P.Sethunathan et.al, [6] conducted aerodynamic analysis of super critical aero foils like 0406,0412,0706 and 1006 using ICEM-CFD to compare their coefficient of lift and coefficient of drag at various angles of attack. Also pressure distribution was measured to verify the effects of aerofoil structure in subsonic speed at a flow velocity of 25 m/s. From this work, it was concluded that super critical aerofoil 0706 performed better in terms of drag reduction and lift increase when compared with other aero foils.

CFD analysis on supercritical aerofoil SC20412 has been done by N.Vinayaka et.al, [7] to understand the performance and normal shock wave behavior at transonic velocity regime at high altitude .The work was performed at 2% and 10% Turbulent Intensity levels at Mach 0.8 and Mach 0.9 with each at 0<sup>0</sup> and 5<sup>0</sup> Angle of Attack. It was concluded that the Co-Efficient of Lift of the aerofoil decreases as the Mach number reaches 0.9 from 0.8. As the angle of attack increases coefficient of lift increases. The results also showed weak Mach wave and a normal shock wave on the lower and upper surface respectively at Mach 0.8. The normal shock wave starts moving towards leading edge as the angle of attack increases. Shock wave started moving away from the leading edge as the Mach number increased. The shock wave moves towards the leading edge as the turbulence intensity increases.

Novel Kumar Sahu and Shadab Imam [8] conducted transonic flow analysis over NACA 0012 aerofoil using Spalart-Allmaras and k- $\omega$  turbulence model and PRESTO solution technique to determine skin friction coefficient, drag coefficient and lift coefficient for variations of angle of attack and Mach number. From this work, it was concluded that lift coefficient increases significantly as the angle of attack increases but there is a limitation of increasing angle of attack i.e. the angle of attack starts converging after 16<sup>o</sup>.As the Mach number increases, shock waves appear in the flow field, getting stronger as the speed increases.

Anderson, Jr.J.D. [9] has clearly given the fundamental aspects of Fluid Dynamics. He has mentioned the physics of continuity, momentum and energy equations in his book.

The main purpose of this analysis is to carryout computational flow analysis on NACA SC (2)-0714 super critical airfoil. The transonic flow regime over the NACA SC (2)-o714 airfoil at Reynolds number (0.36\*10<sup>6</sup>) will be simulated. This project concentrates on determination of coefficient of drag, flow separation on NACA SC (2)-0714 corresponding to the flow is computed using fluent in ANSYS 2019 R3 and also comparison of the pressure drag values of super critical airfoil with NACA SC (2)-0414 airfoil.

### 1.1 OBJECTIVE

This work consists of the following major categories which encompasses

- To study on NACA SC (2)-0714 airfoil.
- To carry out simulation to find out the pressure and velocity distribution contours at different Mach numbers with different angles of attack.
- To carry out simulation to find out the drag and lift coefficients at different Mach numbers with different angles of attack.

It is realized that a larger quantum of work is required to make the study more meaningful, this project was largely aimed at gaining a basic understanding and aerodynamic behavior of NACA SC (2)-0714 airfoil under different Mach numbers and angles of attack and comparison was made with NACA SC (2)-0414 airfoil. .

### 1.2 AEROFOIL DESIGNATION:

The airfoil designation is in the form SC(X)-ABCD, where SC(X) indicates Supercritical (Phase X). The next two digits, AB, designate the airfoil design lift coefficient in tenths (A.B), and the last two digits CD designate the airfoil maximum thickness in percent chord (CD percent).

SC (2)-0714 supercritical (phase 2)--0.7 design lift coefficient, 14 percent thick

SC (2)-0414 supercritical (phase 2)--0.4 design lift coefficient, 14 percent thick

**1.3 PROBLEM DEFINITION:**

Its unique cross-sectional shape delays the onset of wave drag in the transonic speed range and thus allows aircraft to fly faster and more efficiently. The shape of this wing design is characterized by a rounded leading edge and a flat upper surface which delays the development of a shock wave. The rear of the aerofoil features a reflex cambered under- section which helps the wing develop lift at lower airspeeds.

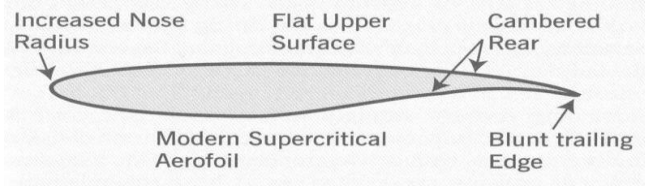


Fig.1: super critical aerofoil



Fig.2: conventional type

Fig.1 shows the NACA SC (2)-0714 supercritical airfoil. The supercritical airfoil is an airfoil that allows an airplane to cruise efficiently at a speed very near Mach one (the speed of sound). The centre portion of the airfoil is nearly flat, and there is distinct downward curve, or cusp, near the trailing edge. The lower side of the forward part of the airfoil is more curved than the upper side. At a particular speed for a given airfoil section, the critical Mach number, flow over the upper surface of an airfoil can become locally supersonic, but slows down to match the pressure at the trailing edge of the lower surface without a shock. However, at a certain higher speed, the drag divergence Mach number, a shock is required to recover enough pressure to match the pressures at the trailing edge. This shock causes transonic wave drag, and can induce flow separation behind it; both have negative effects on the airfoil's performance. Fig.2 shows the conventional aerofoil.

**1.4 SOFTWARE PACKAGES USED**

In this Present Analysis both the airfoils are designed using CATIA V5 software and the complete analysis is carried out in Workbench in ANSYS 2019 R3.

**II. PROBLEM DESCRIPTION**

**2.1 NACA SC (2)-0714 AND NACA SC (2)-0414 AIRFOILS**

**2.1.1 NACA SC (2)-0714**

NACA SC (2)-0714 airfoil is a two dimensional turbulence airfoil. It is designed to delay the preliminary onset of a wave drag. These airfoils are developed in 1960's and tested by NASA engineer Richard Whitcomb. The supercritical airfoil design incorporated in the design of supercritical wing. It produces weak shock wave by comparing to the 0414 series. Due to the formation of weak shock wave drag formation decreases and coefficient lift increases.

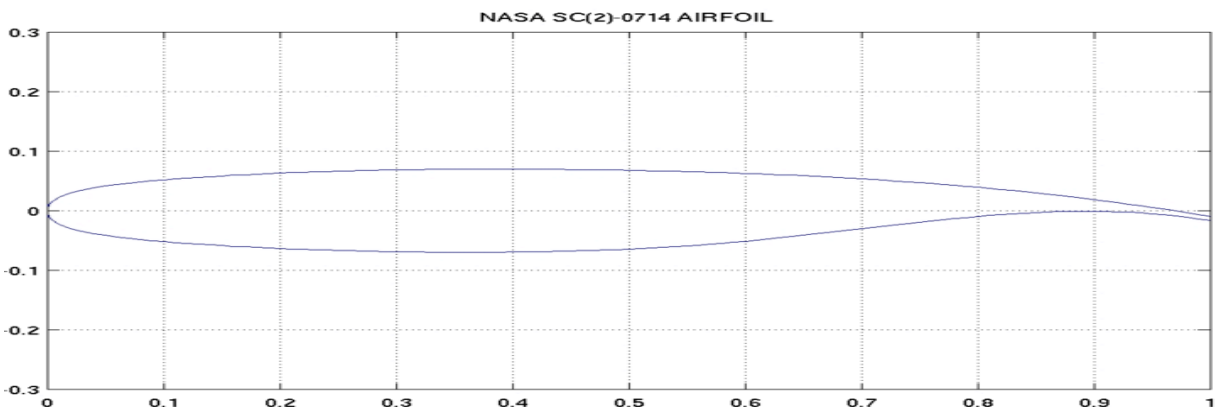


Fig.3: 0714 aero foil

**2.1.2 NACA SC (2)-0414**

NACA SC (2)-0414 airfoil is a typical modern supercritical airfoil and is described as one of series of airfoils which is designed for basic flutter tests. The model of this airfoil is similar to the model of NACA 0012 and NACA 64010.

The NACA SC (2)-0414 airfoil is an aft loaded supercritical airfoil with significant aft camber and develops a shock further aft. at a transonic flow of a region boundary layer forms normally and reduction of drag occurs by the weak shock waves. The separation of boundary layer is very less by comparing to the conventional airfoils.

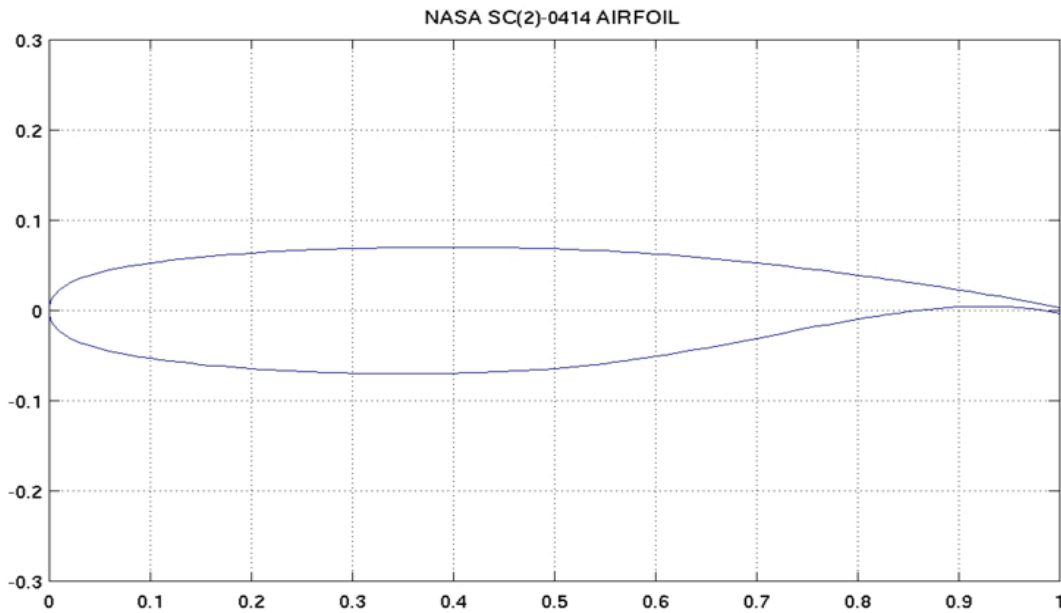


Fig.4: 0414 aero foil

Table 1: Aerofoil Data

Thickness	13.9%
camber	1.5%
Lower flatness	9.4%
Leading edge radius	2.9%
Coefficient of Lift(Max)	1.442
Max. Coefficient of Lift angle	15 degree
Lift/ Drag Max.	27.881
Max.Lift/ Drag angle	4.5 degree

## 2.2 OPERATING CONDITIONS

**K-EPSILON (K-ε) Turbulence model** - The k-epsilon (k-ε) turbulence model is a one-equation model that solves a modeled transport equation for the kinematic eddy turbulent viscosity. The k-epsilon (k-ε) model was used for aerodynamic analysis of SC (2) 0714 and SC (2) 0414 aero foils.

**Reynolds Number** - The Reynolds number is a critical parameter used to characterize different flow regimes within a given fluid, such as laminar or turbulent flow.

**Mach number** - In fluid dynamics, the Mach number is a dimensionless quantity representing the ratio of flow velocity past a boundary to the local speed of sound.

**Angle of Attack** - Angle of attack is the angle between the oncoming air or relative wind and a reference line on the airplane or wing.

## 2.3 BOUNDFARY CONDITIONS

Table2: Boundary Conditions

Input	value
Mach Number	0.7,0.8,1,1.2
Operating temperature	300 K
Operating pressure	65000 Pascals
Turbulence Model transaction	Viscous (k-epsilon)
Density of fluid	$1.225 \text{ kg/m}^3$
Kinematic viscosity	$1.4607 \times 10^{-5}$
Reynolds number	Varies by the type of flow( laminar or turbulent)
Angle of Attack(AOA)	0.3,-3 degrees
Fluid	Air as an ideal

### III. MATERIALS AND METHODS

#### 3.1 MODELING

3.1.1 .The NACA SC (2)-0714 airfoil is generated in CATIA with chord length 160mm, thickness 14%, length of the airfoil 240mm. Geometry wing in CATIA as shown in figure below.

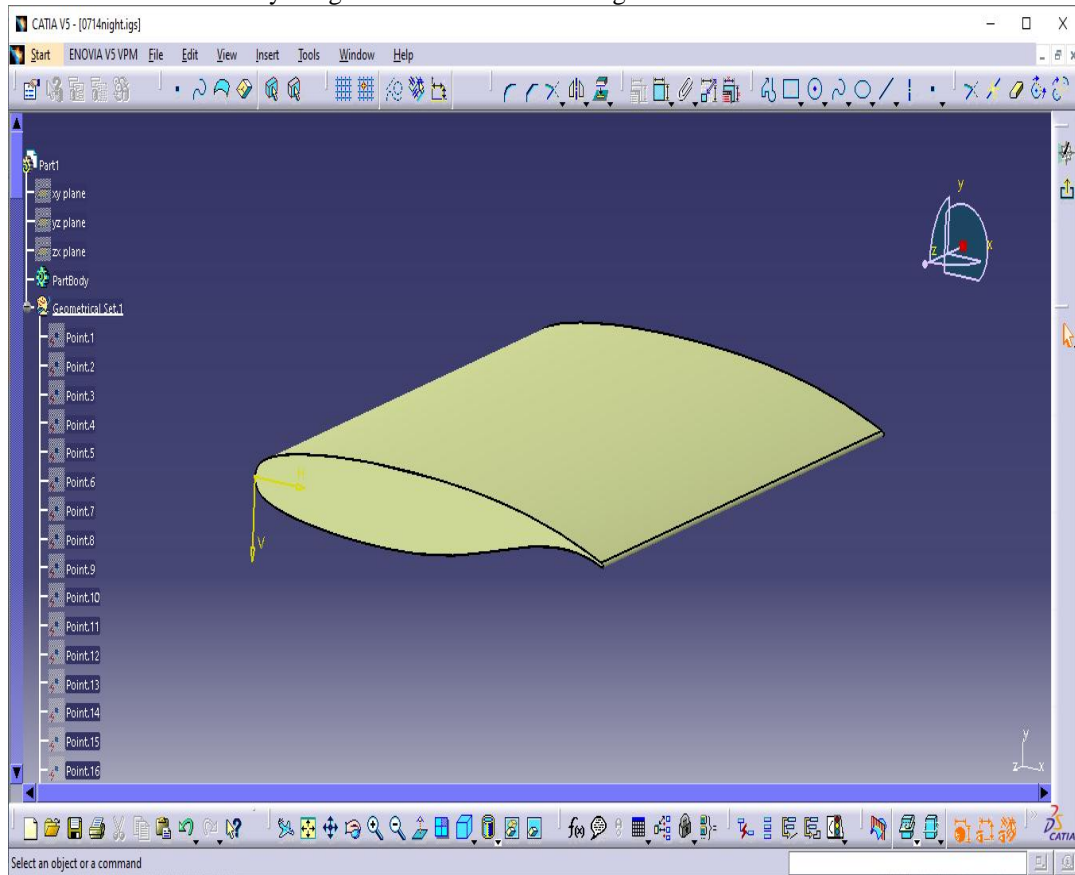


Fig.5: airfoil design

3.1.2 .The generated wing is imported to the custom system in ANSYS WORKBENCH of fluid flow (FLUENT). The generated airfoil is rotated and domain is created using polygon plane. Sketching and Boolean operations are performed on the aerofoil to subtract wing from the domain. Then edge sizing and meshing was done with mapped face. Sections are named as wall for all four sides and as airfoil for model.

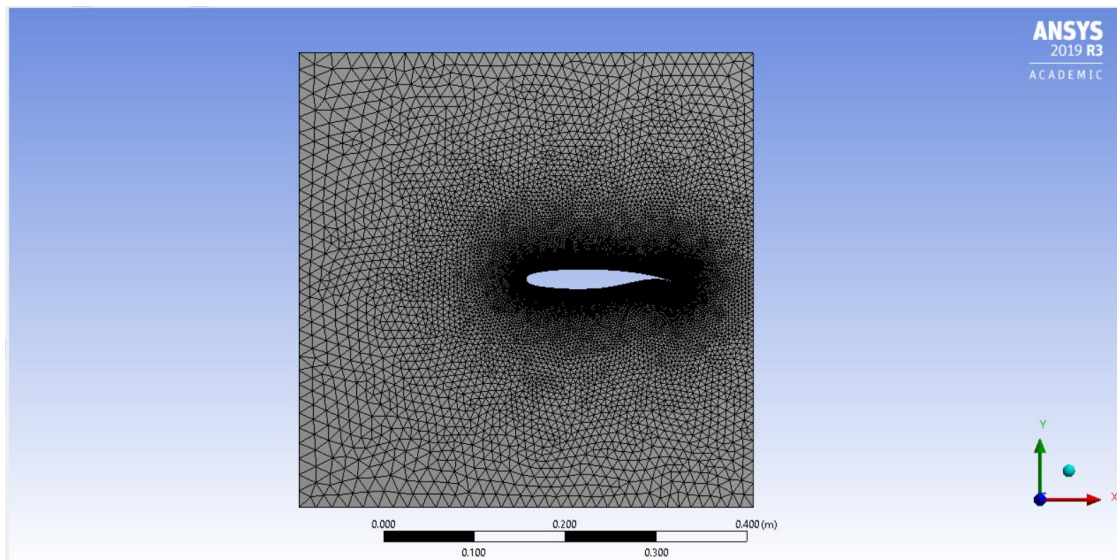


Fig.6: mesh generation

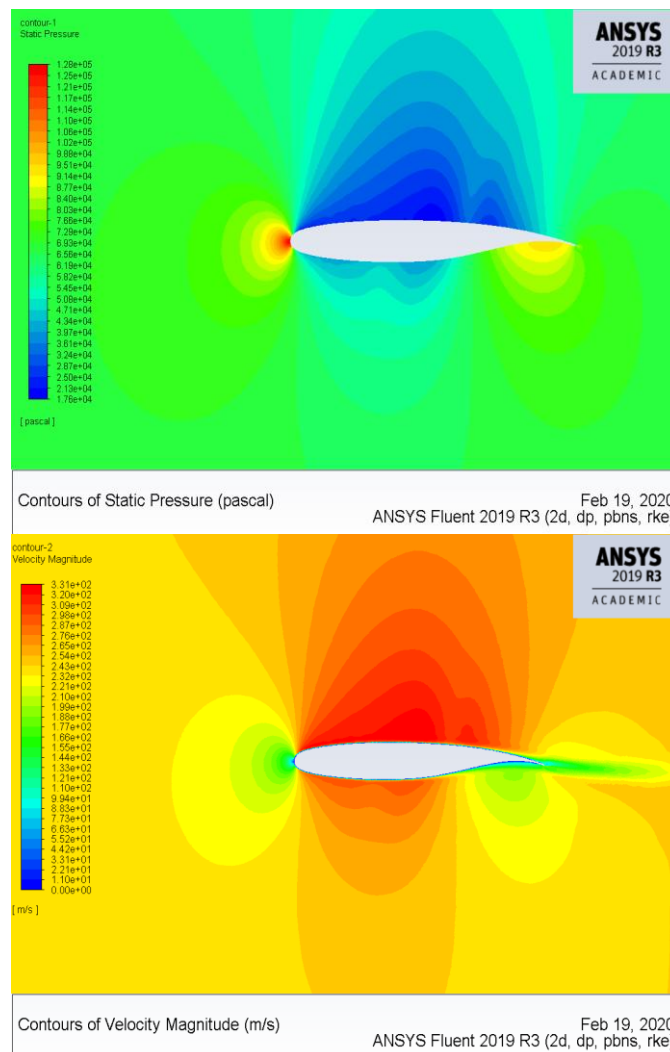
The flow was set up for 2D with Double Precision and display option of mesh after reading. Fluent Launcher is used to check the geometry and select the type as pressure-based, the velocity formulation as absolute and select the time as steady. K-epsilon viscous model was selected with standard constants and material as air. The boundary conditions used here are all free four edges named as wall and the model as aerofoil. The defined boundary conditions are of pressure 65000 Pascal, Mach number 0.8, turbulent intensity 5% and turbulent viscosity ratio 10. And the reference values are of area 1 m<sup>2</sup> density 1.9 m3/kg, enthalpy 40411J/kg, temperature 300K, velocity 277m/s and ratio of specific heats 1.4. Report properties like Name-drag-cd, Type-drag, Surface name-aerofoil, Average over-1and initialization standard methods to compute from wall are included in the analysis. Run calculations are performed for 200 numbers of iterations and data file quantities like turbulent kinetic Energy, static pressure, density, Mach number are specified.

**NOTE:** same procedure has been followed for simulation of 0414 aerofoil in the transonic range of Mach numbers.

#### IV. RESULTS & DISCUSSIONS

The results here are shown pressure and velocity contours of a 0714 and 0414 airfoil at different mach numbers and different angles of attack (AoA) for input boundary conditions as mentioned.

4.1 Pressure and velocity Contours of 0714 aerofoil at 0.7 Mach number for angles of attack 0°, 3° and -3°.



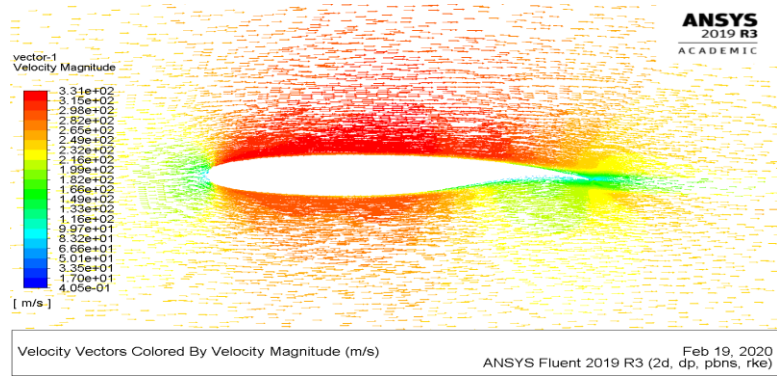
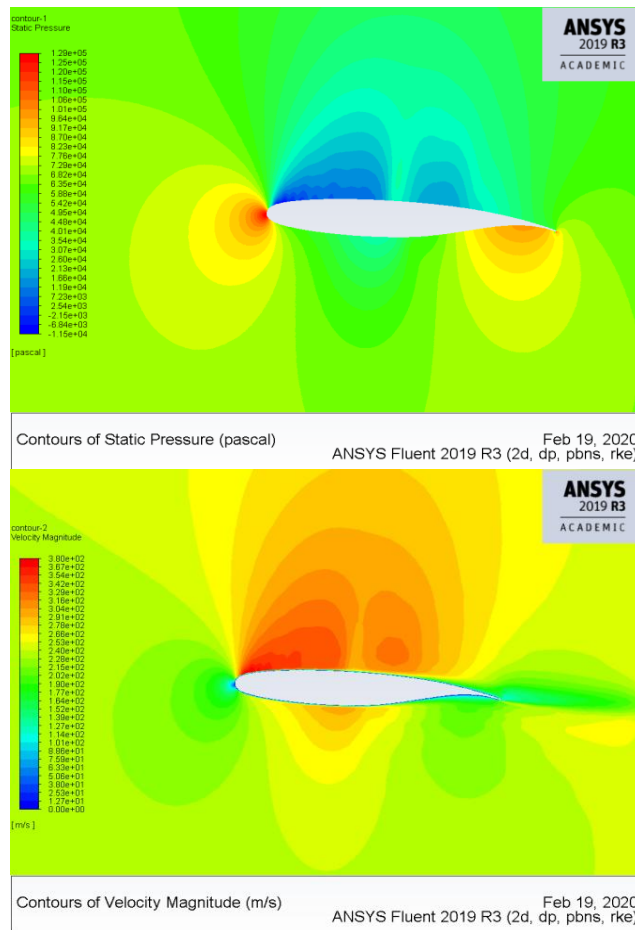


Fig.7: 0.7 Mach and  $0^0$  Angle of Attack (AOA)

Fig.7 shows the pressure and velocity distribution over 0714 aerofoil at Mach number 0.7 and at  $0^0$  AOA. It was observed from the above images that the flow over the supercritical aerofoil is turbulent at trailing edge than at leading edge and the boundary layer separation is gradually increases.



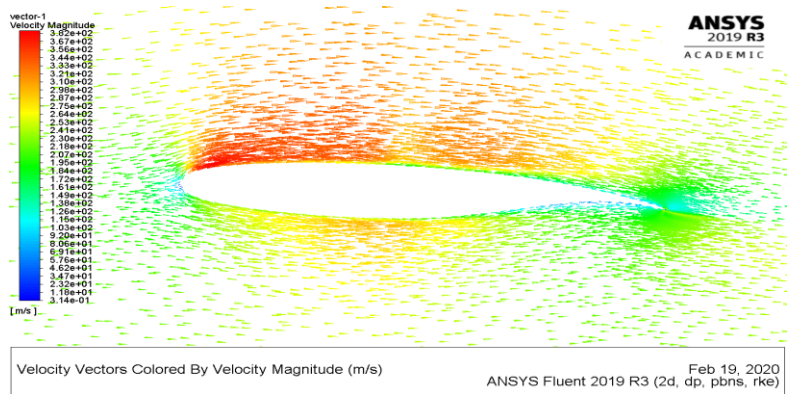
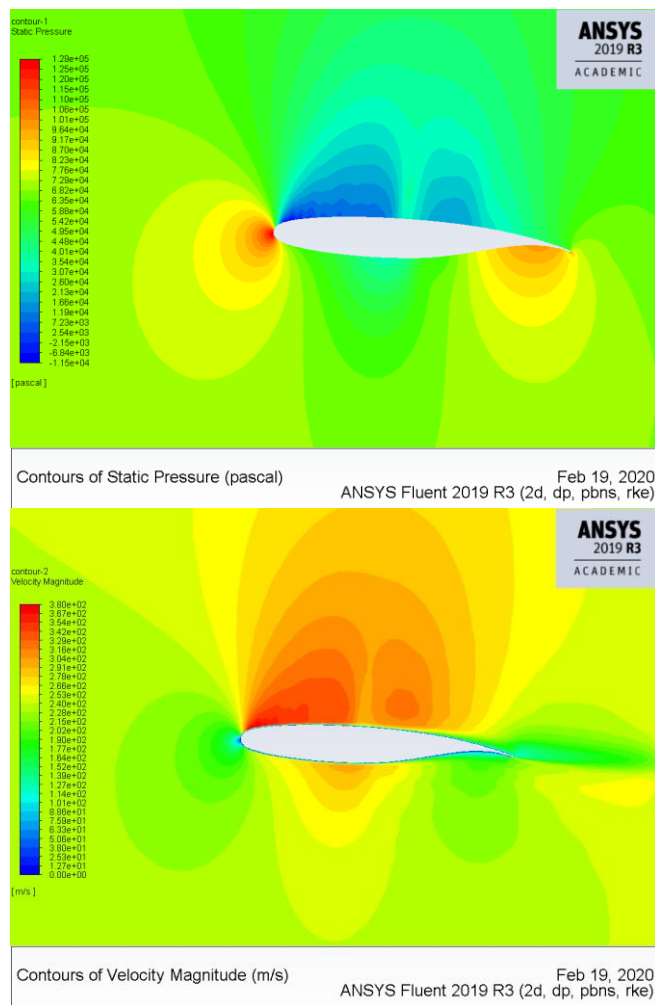


Fig.8: 0.7 Mach and 3<sup>0</sup> Angle of Attack (AOA)

Fig.8 shows the pressure and velocity distribution over 0714 aerofoil at Mach number 0.7 and at 3<sup>0</sup> AOA. It was observed from the above images that the flow over the supercritical aerofoil is turbulent at trailing edge than at leading edge and the boundary layer separation is gradually increases. Almost similar behavior is as that of AOA 0<sup>0</sup>.



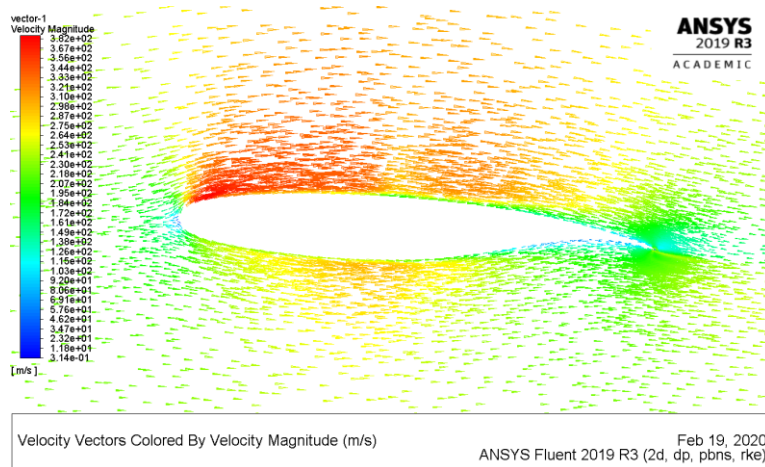


Fig.9: 0.7 Mach and  $-3^{\circ}$  Angle of Attack (AOA)

Fig.9 shows the pressure and velocity distribution over 0714 aerofoil at Mach number 0.7 and at  $-3^{\circ}$  AOA. It was observed from the above images that the flow over the supercritical aerofoil is turbulent at trailing edge than at leading edge and the boundary layer separation is gradually increases. Also static pressure and contours were drawn for other Mach numbers 0.8,1, 1.2 over NACA SC(2)0714 super critical aerofoil using Ansys Fluent at different angles of attack  $0^{\circ}, 3^{\circ}$  and  $-3^{\circ}$ . It was observed from the images of pressure and velocity contours that the flow over the supercritical aerofoil is turbulent at trailing edge than at leading edge and the boundary layer separation is gradually increases for Mach numbers 0.8,1, 1.2 at angles of attack  $0^{\circ}, 3^{\circ}$  and  $-3^{\circ}$ .

#### 4.2 Pressure and velocity Contours of 0414 airfoil at 0.7 Mach number for angles of attack $0^{\circ}, 3^{\circ}$ and $-3^{\circ}$ .

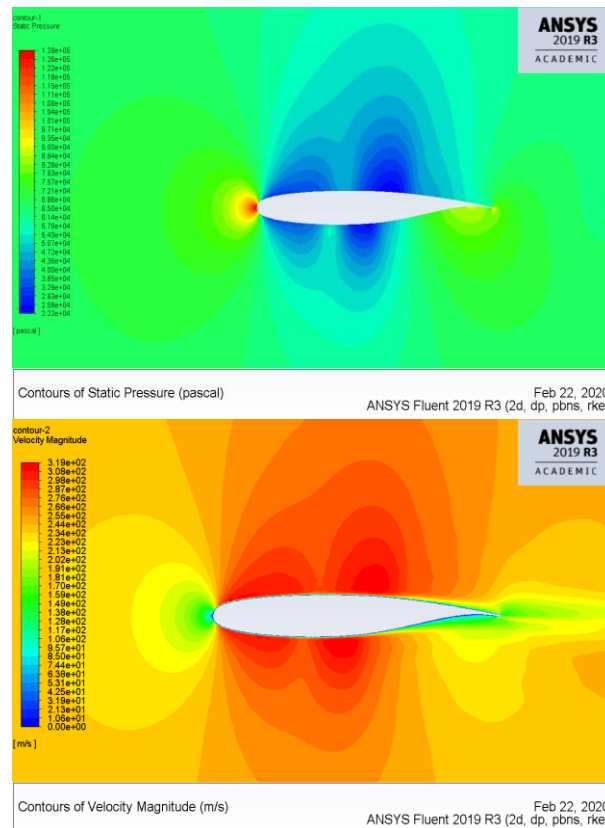


Fig.10: 0.7 Mach and  $0^{\circ}$  Angle of Attack (AOA)

Fig.10 shows the pressure and velocity distribution over 0414 aerofoil at Mach number 0.7 and at  $0^{\circ}$  AOA. The flow over supercritical airfoil was obtained by performing CFD analysis & it was observed from the above images of pressure and velocity differences that the flow over the trailing edge of supercritical airfoil is turbulent than at leading edge and the boundary layer separation is gradually increases.

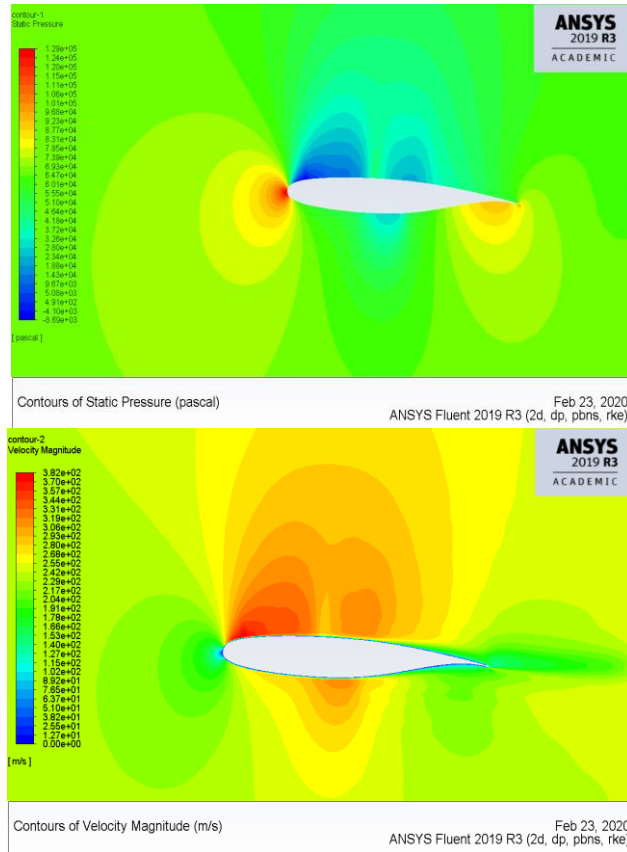


Fig.11: 0.7 Mach and 3<sup>0</sup> Angle of Attack (AOA)

Fig.11 shows the pressure and velocity distribution over 0414 aerofoil at Mach number 0.7 and at 3<sup>0</sup> AOA. The flow over supercritical airfoil was obtained by performing CFD analysis & it was observed from the above images of pressure and velocity differences that the flow over the trailing edge of supercritical airfoil is turbulent than at leading edge and the boundary layer separation is gradually increases.

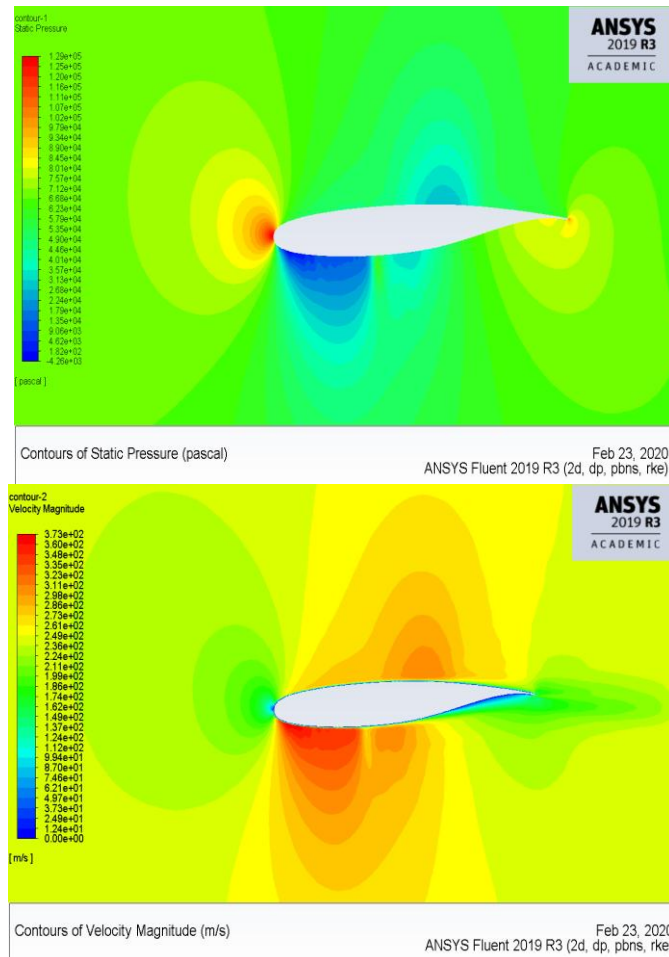


Fig.12: 0.7 Mach and  $-3^{\circ}$  Angle of Attack (AOA)

Fig.12 shows the pressure and velocity distribution over 0414 aerofoil at Mach number 0.7 and at  $-3^{\circ}$  AOA. The flow over supercritical airfoil was obtained by performing CFD analysis & it was observed from the above images of pressure and velocity differences that the flow over the trailing edge of supercritical airfoil is turbulent than at leading edge and the boundary layer separation is gradually increases.

Also static pressure and contours were drawn for other Mach numbers 0.8,1, 1.2 over NACA SC(2)0414 super critical aerofoil using Ansys Fluent at different angles of attack  $0^{\circ}, 3^{\circ}$  and  $-3^{\circ}$ . It was observed from the images of pressure and velocity contours that the flow over the supercritical aerofoil is turbulent at trailing edge than at leading edge and the boundary layer separation is gradually increases for Mach numbers 0.8,1, 1.2 at angles of attack  $0^{\circ}, 3^{\circ}$  and  $-3^{\circ}$ .

Table 3: Aerodynamic parametric values for both the aero foils at Mach number 0.7 and  $0^{\circ}$  AoA

Parameter	NACA SC(2) 0714 aerofoil	NACA SC(2) 0414 aerofoil
LIFT FORCE	4717.87	2259.27
DRAG FORCE	271.101	216.81
LIFT COEFFICIENT	0.0827	0.0396
DRAG COEFFICIENT	0.00475	0.00380

Table 4: Aerodynamic parametric values for both the aero foils at Mach number 0.7 and  $3^{\circ}$  AoA

Parameter	NACA SC(2) 0714 aerofoil	NACA SC(2) 0414 aerofoil
LIFT FORCE	7201.16	5161.42
DRAG FORCE	573.32	395.29
LIFT COEFFICIENT	0.126	0.091
DRAG COEFFICIENT	0.0101	0.0069

**Table 5: Aerodynamic parametric values for both the aero foils at Mach number 0.7 and -3° AoA**

Parameter	NACA SC(2) 0714 aerofoil	NACA SC(2) 0414 aerofoil
LIFT FORCE	1336.56	-717.51
DRAG FORCE	161.54	177.66
LIFT COEFFICIENT	0.0234	-0.0125
DRAG COEFFICIENT	0.00028	0.0031

TABLES 3,4,5 shows the lift and drag coefficients of both supercritical aero foils at the Mach number 0.7 for angles of attack 0°, 3°, -3° respectively. It was observed that lift coefficient values of NACA SC (2) 0714 aerofoil are higher than that of NACA SC (2) 0414 aerofoil for all angles of attack and drag coefficient values are comparable with each other. Here drag values are smaller and hence there is a limited possibility of formation of shock wave.

**Table 6: Aerodynamic parametric values for both the aero foils at Mach number 0.8 and 0° AoA**

Parameter	NACA SC(2) 0714 aerofoil	NACA SC(2) 0414 aerofoil
LIFT FORCE	5137.73	2874.46
DRAG FORCE	652.37	577.21
LIFT COEFFICIENT	0.068	0.0386
DRAG COEFFICIENT	0.0087	0.018

**Table 7: Aerodynamic parametric values for both the aero foils at Mach number 0.8 and 3° AoA**

Parameter	NACA SC(2) 0714 aerofoil	NACA SC(2) 0414 aerofoil
LIFT FORCE	10906.91	6826.29
DRAG FORCE	1403.52	864.19
LIFT COEFFICIENT	0.1464	0.0916
DRAG COEFFICIENT	0.0188	0.0116

**Table 8: Aerodynamic parametric values for both the aero foils at Mach number 0.8 and -3° AoA**

Parameter	NACA SC(2) 0714 aerofoil	NACA SC(2) 0414 aerofoil
LIFT FORCE	1795.03	-1162.93
DRAG FORCE	640.59	712.035
LIFT COEFFICIENT	0.241	-0.0156
DRAG COEFFICIENT	0.0086	0.00956

TABLES 6,7,8 shows the lift and drag coefficients of aero foils at the Mach number 0.8 for angles of attack 0°, 3°, -3° respectively. Here also it was observed that lift coefficient values of NACA SC (2) 0714 aerofoil are higher than that of NACA SC (2) 0414 aerofoil for all angles of attack and drag coefficient values are comparable with each other.

**Table 9: Aerodynamic parametric values for both the aero foils at Mach number 1 and 0° AoA**

Parameter	NACA SC(2) 0714 aerofoil	NACA SC(2) 0414 aerofoil
LIFT FORCE	2446.94	633.85
DRAG FORCE	2887.09	2626.71
LIFT COEFFICIENT	0.21	0.0054
DRAG COEFFICIENT	0.0248	0.0225

**Table 10: Aerodynamic parametric values for both the aero foils at Mach number 1 and 3° AoA**

Parameter	NACA SC(2) 0714 aerofoil	NACA SC(2) 0414 aerofoil
LIFT FORCE	7189	5009.84
DRAG FORCE	3095.05	2891.81
LIFT COEFFICIENT	0.0617	0.0431
DRAG COEFFICIENT	0.026	0.0248

TABLES 9 and 10 show the lift and drag coefficients of both the aero foils at the Mach number 1 for angles of attack 0°, 3° respectively. Here also it was observed that lift coefficient values of NACA SC (2) 0714 aerofoil are higher than that of NACA SC (2) 0414 aerofoil for all angles of attack and drag coefficient values are comparable with each other.

**Table 11: Aerodynamic parametric values for both the aero foils at Mach number 1.2 and 0° AoA**

Parameter	NACA SC(2) 0714 aerofoil	NACA SC(2) 0414 aerofoil
LIFT FORCE	2310.35	715.06
DRAG FORCE	4043.63	3700.4
LIFT COEFFICIENT	0.013	0.0042
DRAG COEFFICIENT	0.024	0.0221

Table 12: Aerodynamic parametric values for both the aero foils at Mach number 1.2 and 3°AoA

Parameter	NACA SC(2) 0714 aerofoil	NACA SC(2) 0414 aerofoil
LIFT FORCE	8446.31	5814.67
DRAG FORCE	4494.02	3947.064
LIFT COEFFICIENT	0.050	0.034
DRAG COEFFICIENT	0.026	0.0235

TABLES 11 and 12 show the lift and drag coefficients of both the aero foils at the Mach number 1.2 for angles of attack 0°, 3° respectively. Here also it was observed that lift coefficient values of NACA SC (2) 0714 aerofoil are higher than that of NACA SC (2) 0414 aerofoil for all angles of attack and drag coefficient values are comparable with each other.

There is a wave drag due to formation of shock waves which transforms the energy produced from the propulsion system of aircraft to the heat energy. This leads to loss of energy. The drag values of NACA SC(2) 0714 are less in transonic speed because of 0714 aero foil having blended trailing edge than the 0414 aerofoil.

## V. CONCLUSION

The following conclusions are drawn from the CFD analysis of the flow field around supercritical airfoils NACA SC (2)0714 and NACA SC (2)0414 with different mach numbers at different Angle of attack (AOA).

- It was found that the static pressure on the lower surface of the airfoil at leading edge is greater than static pressure on the upper surface of the aerofoil.
- It was observed from the images of pressure and velocity contours that the flow over the supercritical aerofoil is turbulent at trailing edge than at leading edge and the boundary layer separation is gradually increases for Mach numbers 0.7, 0.8, 1, 1.2 at angles of attack 0°, 3° and -3°.
- It was observed that lift coefficient values of NACA SC (2) 0714 aerofoil are higher than that of NACA SC (2) 0414 aerofoil for all angles of attack and drag coefficient values are comparable with each other for transonic Mach numbers 0.7, 0.8, 1, and 1.2.
- The 0714 airfoil has flattened upper surface with large leading edge radius and blended trailing edge; 0414 airfoil also having flattened upper surface with large leading edge radius and having small blended trailing edge compared to 0714 airfoil. Hence NACA SC(2)0714 Produces weaker shock waves at leading edge than the shock waves at leading edge of NACA SC (2)0414.
- The performance of NACA SC (2) 0714 super critical aerofoil was better than the NACA SC (2)0414 in the transonic region with respect to aircraft speed, strength and safety.

## REFERENCES

- [1]. Ravi Kumar T and Dr.S.B.Prakash, Aerodynamic analysis of super critical NACA SC (2) - 0714 airfoil using CFD, International Journal of Advanced Technology in Engineering and Science, 2 (7), 2014, 285-293.
- [2]. Rubel et.al, Comparison of aerodynamics characteristics of NACA0015 & NACA4415 Aerofoil blade, International Journal of Research-G., 5(11), 2017, 187-197.
- [3]. M.Umapathi and Neelesh Soni, Comparative analysis of Air foil NACA2313 and NACA7322 using Computational Fluid Dynamics Method, International Journal of Science Progress and Research, 12(4), 2015, 193-198.
- [4]. Haydar Kepecki, Comparative numerical Aerodynamics performance analysis of NACA0015 and NACA4415 Airfoils, International Journal of Engineering Science & Information Technology, 2(1), 2022, 144-151.
- [5]. Harish Kumar K.et.al., CFD Analysis of RAE 2822 super critical airfoil at transonic Mach speeds, International Journal of Research in Engineering and Technology, 4(9), 2015, 256-262.
- [6]. Sethunathan P., et.al, Analysis of aerodynamic characteristics of a super critical airfoil for low speed aircraft, International Journal of Research in Engineering and Technology, 3 (6), 2014, 179-183.
- [7]. Vinayaka.N.et.al., High altitude transonic aerodynamics of Super critical Airfoil at different turbulence levels, Journal of Advanced research in Fluid Mechanics and Thermal sciences, 60(2), 2019, 283-295.
- [8]. Novel Kumar Sahu and Shadab Imam, Analysis of Transonic Flow over an Airfoil NACA0012 using CFD, International Journal. of Innovative Science, engineering and Technology, 2(4), 2015, 379-388.
- [9]. John D Anderson Jr., Fundamentals of aerodynamics (Newyork, McGraw Hill, 1991).

M. Sri Rama Murthy, et. al. "Aerodynamic analysis of NACA SC (2) -0714 and NACA SC (2)-0414 super critical aero foils –a comparative study." *International Journal of Engineering Science Invention (IJESI)*, Vol. 11(11), 2022, PP 15-27. Journal DOI- 10.35629/6734